

Multi-Domain Statistical Diagnosis and Yield Enhancement of Liquid Crystalline Polymer based RF Circuits

ABSTRACT

A layout-level multi-domain statistical diagnosis methodology and yield optimization technique for multilayer RF passive circuits is presented. The circuits are composed of quasi-lumped embedded inductors and capacitors in Liquid Crystalline Polymer (LCP) substrate. The statistical diagnosis approach is based on layout segmentation, lumped element modeling, sensitivity analysis and extraction of probability density function using convolution methods. The statistical analysis takes into account the effect of thermo-mechanical stress effects and process variations that are incurred in batch fabrication. Appropriate transformation techniques for analysis with non-Gaussian distributed parameters have also been discussed. Yield enhancement methods based on constraint-based convex optimization have also been presented. The results show good correlation with measurement/electromagnetic (EM) data.

Keywords

Bandpass filter, Liquid Crystalline Polymer (LCP), parametric yield, RF synthesis, statistical diagnosis, warpage modeling.

1. INTRODUCTION

The design of wireless circuits for RF frequencies require precise values of passive components which is partially satisfied due to manufacturing variations, resulting in yield loss. In addition, the integration of passives in multilayer RF circuits requires reliability estimation in order to maximize yield in batch fabrication. However fault detection and diagnosis for RF circuits after manufacturing is a time-consuming step in the design cycle. The focus of this paper is the application of statistical methods and mechanical models that enable diagnosis and yield enhancement of batch fabricated RF circuit layouts for new technologies, which significantly reduces the design cycle time.

In RF designs, the physical effects of layout, such as electromagnetic coupling and parasitics affect circuit performance. Therefore statistical analyses of RF circuits that are based on circuit simulators are fast but do not provide accurate results. The conventional method to study the effect of component variations on system performance is to perform Monte Carlo analysis. However, Monte Carlo technique for EM simulations can be time and memory-intensive. In addition, Monte Carlo analysis does not provide diagnosis capability. Clearly there is a need for time-efficient multi-domain diagnosis of RF circuits in prototype designs as well as in volume production based on batch fabrication. This paper includes the effect of thermo-mechanical



Fig.1 Photograph of batch-fabricated bandpass filters on a single panel; each block represents a filter

stresses and dielectric variations incurred in large panel fabrication by implementing warpage models of LCP boards in sensitivity analysis. The analysis is “multi-domain” since it considers the effects of process variations at the circuit and board level that is critical to reliable yield estimation in a batch process.

In statistical analysis of sensitivity data, many of the parameters are statistically related, thus requiring the use of the parameters’ correlation coefficient matrix. Since the methods for generating arbitrary sets of statistical parameter data is based on multivariate analysis, transformation of non-Gaussian data to the Gaussian/normal distribution domain is critical. Also, use of Monte Carlo simulations becomes computationally expensive due to the large number of SPICE simulations that needs to be performed at each stage. This paper demonstrates the use of surface response methods to extract statistical distributions of performance measures.

Extensive literature exists on circuit-level design centering and yield optimization for IC fabrication. Statistical design centering approach to minimax circuit design has been shown in [1]. The method focused on yield optimization based on *circuit level* parameters rather than *layout*. Earlier work on *circuit-level* design centering led to the development of algorithms based on convex optimization and radial exploration methods [2], [3]. *Parasitic-aware* post-optimization design centering for RF Integrated Circuits based on simulated annealing [4] reduces iterations in *design optimization* but the work does not focus on *diagnosis*. *Network-level* design centering based on piecewise ellipsoidal approximation has been shown in [5]. Clearly, the focus of most of the prior work has been *design centering* using *circuit parameters* and not *layout-level diagnosis* of RF designs for *large-panel* fabrication.

2. PROPOSED METHODOLOGY

Fig.2 shows the flow diagram of the proposed statistical analysis, diagnosis, and yield enhancement methodology. The process begins by identifying key performance measures and significant design parameters based on sensitivity analysis through circuit/EM simulations (using layout segmentation). To account for thermo-mechanical stress effects incurred in large panels, warpage model of the board is included in the sensitivity analysis.

Regression analysis is used to map multiple performance measures to physical and process parameters. Although, this method is not suitable for broadband mapping, it can be used for fast characterization in *small* (<5%) statistical variation ‘space’, which is the case for statistical diagnosis. Yield analysis is performed by computing the joint probability distribution function (JPDF) of the performance measures. Parametric causes of the unacceptable performance of an individual system can then be searched by using the information acquired from the statistical analysis thereby performing layout-level diagnosis.

Convolution methods are used to compute statistical distributions of performance measures for Gaussian data. Response surface analysis/transformation methods are used to apply similar statistical analysis with non-Gaussian data. The estimates are realistic as the statistical analyses are multi-domain, taking into account the electrical parametric variations at the circuit level and mechanical variations at the board level. Convex optimization has been employed to optimize a *limited* but *critical* set of design parameters to improve yield.

3. EMBEDDED PASSIVES IN LCP SUBSTRATE

LCP is a low loss material ($\tan\delta=0.002$) with a relative permittivity (ϵ_r) of 2.95. The material properties are practically invariant upto 20 GHz with negligible moisture absorption (0.04%). As a result, the embedded passives provide high Q and stable component values across a large frequency range [6]. The process is low cost due to the use of large area manufacturing, as shown in Fig. 1. Furthermore, the process is low temperature (200°C) and large area boards (12”X18”) can be batch-fabricated, making it compatible with printed wiring board (PWB) infrastructure. High performance and miniaturized filters, low noise amplifiers and voltage-controlled oscillators functional from 500 MHz to 10 GHz using embedded inductors and capacitors in LCP dielectric material have been shown in [6],[7]. The 3-D layout of a dualband filter is shown in Fig.3. The design cross-section (c.s.) has 2 inner metal layers for passives embedded in LCP (1 mil thick) in the middle of the c.s. In addition, top and bottom ground planes are 73 mils from each other and provide electromagnetic shielding.

4. STATISTICAL ANALYSIS

To map process variations to performance, EM simulations are planned using Design Of Experiment (DOE) principles with the following steps a) for each experiment, the filter component values are applied to the *complete* lumped-element model in the circuit simulator namely Agilent’s Advanced Design System (HP-ADS) to obtain filter performance; b) filter performance is related to manufacturing variations and; c) parametric yield is computed using JPDFs of the filter performance. In this paper, design parameters are varied only within their statistical variation ranges.

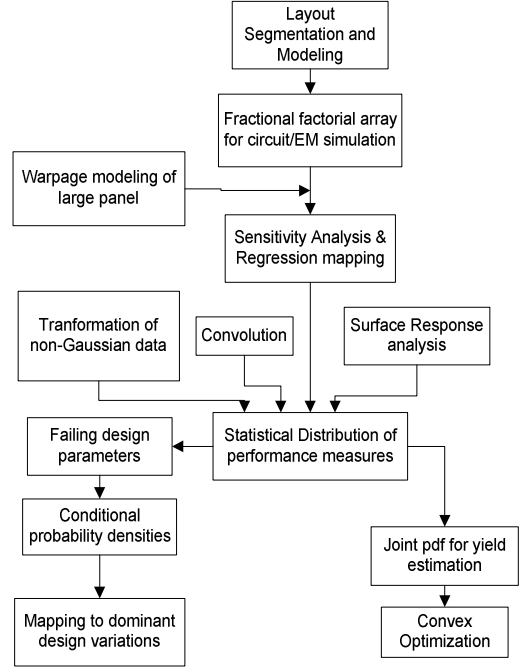


Fig.2 Flowchart for the proposed methodology

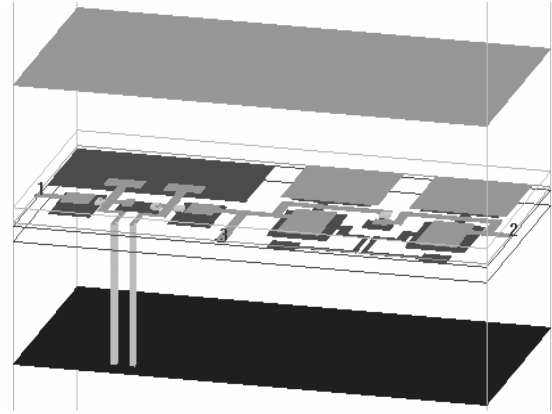


Fig.3 3-D layout of the dualband filter stackup

Therefore, third and higher order effects were ignored. Eqn.1 shows the quadratic model for n design parameters:

$$y = \beta_0 + \sum_{i=1}^n \beta_i x_i + \sum_{i=1}^n \sum_{j=1}^n \beta_{ij} x_i x_j + \varepsilon \quad (1)$$

where y is the approximated response, x 's are design parameters, β_0 is the intercept term, β_i 's are coefficients of first-order effects, β_{ij} are coefficients of second-order effects and ε is the approximation error. A fractional factorial plan has been implemented in this paper. Model parameters of the *components* are extracted from SONNET (a commercial method of moments based EM solver) data. Each performance measure is approximated by linear and piecewise linear terms forming a *regression equation*. For e.g., the following performance measures for the 2.3 GHz filter (Fig.4) are shown in Eqn.2-3:

$$BW_{1dB} = 0.2231 - 0.0426(CC) + 0.0043(C_{resn1}) + 0.0030(U(L) - 0.014(\epsilon_r)) \quad (R^2=0.997) \quad (2)$$

$$f1=2.2525 - 0.0395(\text{resn_C})+ 0.0037(\text{C_match}) - 0.0341(\text{resn_L}) - 0.0044(\epsilon_r) \quad (R^2=0.985) \quad (3)$$

CC, C_resn1, L and C_m1 are the component dimensions (as also shown in Fig.4). The performance variables stands for 1 dB bandwidth and lower cutoff frequency of 1 dB bandwidth. Here R^2 represents regression coefficients and U is the unit step function. R^2 values close to 1 indicates good predictive capability of approximation equations. The lumped-modeling approach works well with designs with less than 5 layers. Since the variations of the layout parameters are independent of each other, the pdf of the performance measures are computed by convolution of the pdfs of the layout parameters. The pdf of the 1 dB bandwidth (BW_1dB) of 2.3 GHz filter is computed as Eqn.4:

$$f(\text{BW_1dB})=\delta(\text{BW_1dB}-0.2231)*(-0.0426(\text{CC}))*f(0.0043(\text{C_resn1}))*f(0.0030(\text{L})U(\text{L}))*f(-0.014(\epsilon_r)) \quad (4)$$

where * is the convolution operator, δ is the impulse function and f stands for the pdf of its argument. The pdf of the piecewise linear (pwl) terms is given by Eqn.5:

$$f(y)=N(y,0,\beta_1)U(y/(-\beta_1)) + N(y,0,|\beta_1+\beta_2)U(y/(\beta_1+\beta_2)); \text{ where } y=\beta_1x + \beta_2xU(x) \quad (5)$$

where β_1, β_2 are regression coefficients of the pwl function y, $N(r,\mu,\sigma)$ is the normal pdf function of random variable r, with mean μ and standard deviation σ . The results correlates well with full-scale Monte Carlo simulations.

5. DUALBAND FILTER

The methodology has been implemented on a dualband filter. The design consists of 2 single-band filters synthesized from 2.45 GHz and 5.5 GHz reference layouts. It consists of two band pass responses centered at 2.3 GHz and 4.25 GHz with bandwidths of 225 MHz and 300 MHz respectively. The layout has a lateral dimension of 6.8 mm X 3.3mm with a cross section of 73 mils. The EM simulation results (using SONNET) are shown in Fig.5.

6. BOARD WARPAGE MODELING

Inclusion of warpage effects in large panels (24"X18") is critical to yield estimates in batch-fabrication. The most straight-forward model for thermo-mechanical stress analysis for the stack-up shown in Fig.3 is a two-layer analytical plate model [9]. The top layer is assumed to be LCP and the bottom layer as prepreg. The

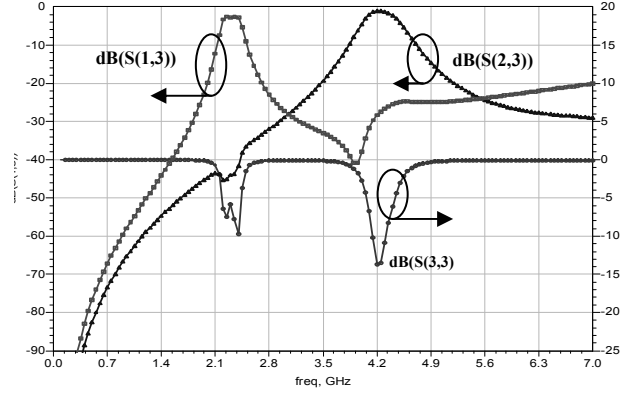


Fig.5 Dual Band Filter Response in EM solver using synthesized geometries

thickness of the LCP layer (h_1) in the model is the combined thickness of all the individual LCP layers (in this case, 1) and similarly for the prepreg layers (h_2). The assumptions is that the two layers have in-plane isotropy with Young's moduli, E_1 and E_2 , Poisson's ratios, ν_1 and ν_2 , and CTEs, α_1 and α_2 . The plate bends with a curvature of κ_R , which is the inverse of the radius of bending (denoted as "R") is given by Eqn. 1:

$$\kappa_R = \frac{D_1}{C_4} 6h_1h_2(h_1 + h_2) \quad (6)$$

where h_1, h_2 denotes the combined thicknesses of the LCP layers, and prepreg layers respectively.

$$C_1 = \overline{E_1^2} h_1^4; \quad C_2 = \overline{E_2^2} h_2^4; \quad C_3 = \overline{E_1 E_2} h_1 h_2 \quad (7)$$

The coefficient C_4 in Eqn. 1 can be obtained by combining the expressions for C_1, C_2, C_3 in Eqn. 2 as shown:

$$C_4 = C_1 + C_2 + \left[C_3 (4h_1^2 + 6h_1h_2 + 4h_2^2) \right] \quad (8)$$

where ΔT is the temperature loading for the process stage whose corresponding curvature is computed. Here the single layer of LCP is 1 mil in thickness which is much smaller compared to the combined thickness of the supporting dielectric layers (73 mils).

Here, in Eqn. 6, D_1 is given by Eqn. 9:

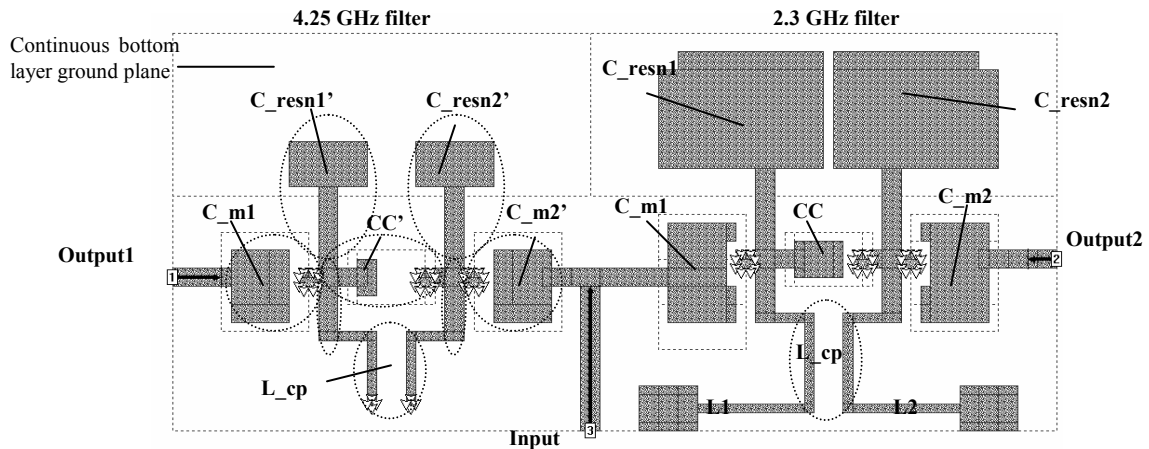


Fig.4 Layout of 2.3 GHz and 4.25 GHz dualband filter

$$D_1 = \overline{E_1 E_2} (\alpha_1 - \alpha_2) \Delta T \quad (9)$$

By using thin-film approximation [9], the curvature is given by:

$$\kappa_R = 6 \frac{\overline{E_1}}{E_2} \frac{h_1}{h_2^2} (\alpha_1 - \alpha_2) \Delta T, \quad h_1 \ll h_2 \quad (10)$$

The maximum warpage displacement (W_L) is given by Eqn. 11 where the curvature K is obtained from previous equation:

$$W_L = L^2 K / 8 \quad (11)$$

where L is the diagonal length from the center of the board. As shown in Fig.7, the warpage of the board grows as the square of the distance from the point where it is held during curing, which in this case, is the center of the board. For warpage levels beyond the dotted line, the statistical trend of circuits is functional failures instead of parametric variations. Accurate finite-element modeling of test structures of just embedded passives using ANSYSTM in similar stack-up has been shown in [10]. In this paper, the filters consist of planar inductors that do not undergo a significant change after deformation, since it does not have any turns in the z direction. In addition, the effect of deformation on inductance is negligible in the frequency range of interest (< 6 GHz). Therefore the effect of capacitance variations is included in the sensitivity analysis.

The mechanical parameter variations are included in the regression equation for the components. For e.g. the regression equation for the resonator capacitor is given by Eqn.12:

$$C_1 = 0.2125 + 0.07611(\epsilon_r) - 0.0982(t) - 0.0231(w_r) \quad (12)$$

where ϵ_r , t and w_r stands for dielectric constant, line width and warpage level respectively. The regression equation is used to find the mean and variance of the capacitance as shown in Eqn 13,14:

$$\mu_{C_1} = 0.2125 + 0.07611\mu_{\epsilon_r} - 0.0982\mu_t - 0.0231\mu_{w_r} \quad (13)$$

$$\sigma_{C_1}^2 = (0.07611)^2 \sigma_{\epsilon_r}^2 + (-0.0982)^2 \sigma_t^2 + (-0.0231)^2 \sigma_{w_r}^2 \quad (14)$$

These multi-domain statistical parameters of the components are used to extract the pdfs of performance measures. The capacitance and Insertion loss of the 2.3 GHz filter (taking into account the mechanical and process variations) have been shown in Fig.6.

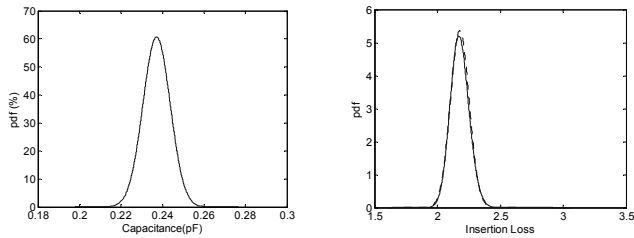


Fig. 6 Unnormalized pdf of capacitance and insertion loss

7. STATISTICAL ANALYSIS WITH NON-GAUSSIAN DATA

The statistical analysis and the convolution methods employed for extraction of the distribution of performance measures requires the data to be in the Gaussian/normal domain. Typical MonteCarlo simulations in circuit analysis consist of applying random variations in the design parameters and performing

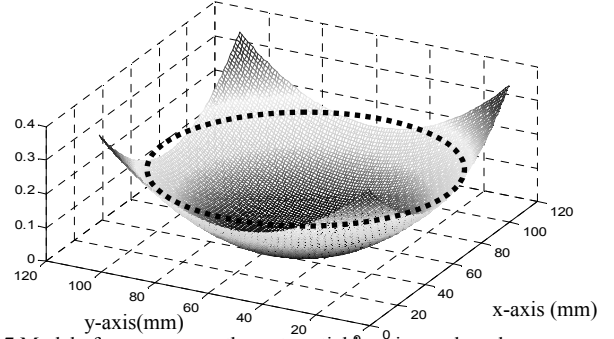


Fig.7 Model of warpage growth w.r.t spatial location on board

SPICE simulations to extract the circuit response. In Section 4, it was shown how convolution methods are used to extract distributions of performance measures from sensitivity data. In this part, response surfaces are extracted from sensitivity data. For random variation of the design/process variables, the corresponding perturbed value of the performance measure can be obtained by using least-square methods to approximate the response surface. Fig.8 shows the response surface for Insertion Loss. Fig. 9a shows the unnormalized pdf of the Insertion Loss of the 2.3 GHz filter in the dualband design by using the response surface while Fig.9b represents the same distribution obtained

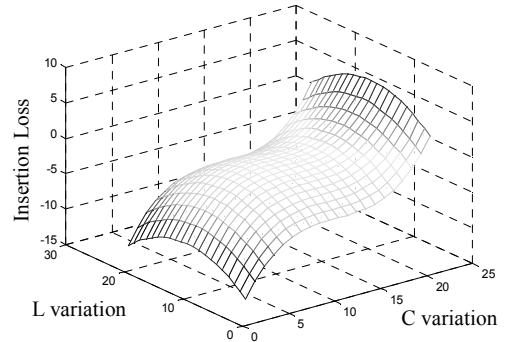


Fig.8 Response surface for Insertion Loss ($\mu \pm 3\sigma$ variation)

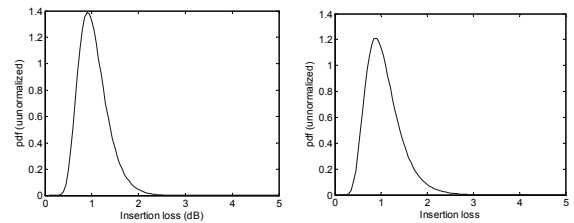


Fig.9 Insertion Loss pdf using (a) response surface and (b) Monte Carlo with non-Gaussian variable

from full-scale Monte Carlo analysis using lognormal design parameters. It can be seen that the response surface based method is in good agreement with Monte Carlo estimation. However, extraction of response surfaces with a large set ($n > 4$) of dominant variation parameters becomes mathematically involved [12]. A simple but powerful alternative is to transform the non-Gaussian raw data into the Gaussian domain. By transformation, it is possible to view normal probability plots, run standard tests for normality, skewness and kurtosis. The square-root ($n=1/2$), lognormal ($n=0$), and reciprocal ($n=-1$) transform from literature [12] are generally sufficient to transform the “skewed” data into

the Gaussian domain. Let x be the original variable, and y its transformed value; then the following transform can be applied:

$$y = a + c(x + b)^n, \quad \text{where } n \neq 0$$

$$y = a + c \log(x + b), \quad \text{where } n = 0$$

If y is the transformed value of x by the function g , i.e. $y=g(x)$ then, as shown by [12],

$$f_x(x) = f_y(g(x)) \left| \frac{dg(x)}{dx} \right| \quad (15)$$

where f denotes a density function. With this new non-Gaussian density function $f_x(x)$ the first and second moments can be expressed as shown in Equation (16),(17):

$$\mu_x = \int_{-\infty}^{\infty} x f_x(x) dx \quad (16); \quad \sigma_x^2 = \int_{-\infty}^{\infty} x^2 f_x(x) dx \quad (17)$$

An important set of transformations are those associated with lognormal distribution. With x lognormal distributed, so that $y=\log x$ is distributed Gaussian, the conversion of log-normal to Gaussian is shown in Eqns. (18), (19) [12]:

$$\mu_y = \log \mu_x - 1/2 \log\left(\frac{\sigma_x^2}{\mu_x^2} + 1\right); \quad (18) \quad \sigma_y^2 = \log\left(\frac{\sigma_x^2}{\mu_x^2} + 1\right) \quad (19)$$

The conversion from Gaussian to lognormal is (20), (21) [12]:

$$\mu_x = \exp[(\mu_y + 0.5\sigma_y^2)]; \quad (20)$$

$$\sigma_x^2 = (e^{\sigma_y^2} - 1) \exp[(2(\mu_y + 0.5\sigma_y^2))] \quad (21)$$

Fig.8 shows the transformation of a lognormal technology variable to Gaussian data form and applying to the aforementioned statistical framework.

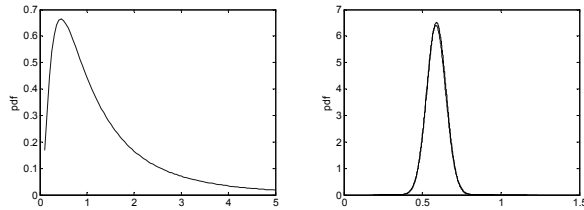


Fig.8 (a) Lognormal distribution and (b) transformed Gaussian distribution of technology variable

8. DIAGNOSIS BASED ON STATISTICAL ANALYSIS

As a result of the statistical variations in design and operational parameters in batch fabrication, some circuits display unacceptable variations in performance measures. For a functional design in this condition, the information extracted from the aforementioned statistical analysis can be utilized as a diagnosis tool. Using the diagnosis methodology, the most probable layout parameters causing the unacceptable variations in performance measures can be systematically searched. For e.g. the linear systems formed by (2), (3) can be used to estimate the variation in the design and operational parameters for the measured variations in system performance. For explaining the diagnosis approach, let $[X]$ and $[Y]$ be the random vectors for m layout parameters and n

performance measures, respectively. If n is less than m , then a unique solution of $[X]$ does not exist for a measured set of unacceptable performance $[Y]$. Hence, the real parameter(s) causing the failure cannot be decided. However since all design parameters are associated with pdfs, the most probable solution can be searched. The conditional pdf of the parameter vector $[X]$ for measured performance y is defined as [8]:

$$f(X|Y=y) = \frac{f(X,Y)}{f(Y)} \quad (22)$$

where $f(X,Y)$ is the joint pdf of the random vector of the design parameters and performance measures $[X^T Y^T]^T$. In (22), $f(Y)$ is the joint pdf of the performance measures. Then, the expected value of $f(X|Y=y)$ is the most probable parameter set causing the failure. Let $\tilde{Y} = [P^1 P^2 \dots P^n]^T$ be the set of unacceptable performance measures. Equations for the performance measures can be rewritten by subtracting the intercept term $\beta_{10}, \beta_{20}, \beta_{30}, \dots, \beta_{n0}$ from \tilde{Y} resulting in

$$Y = \beta X + \varepsilon \quad (23)$$

where X is the parameter vector, and Y, β are defined as the performance vector, $n \times m$ sensitivity coefficient matrix without intercept terms β_{i0} . The error column ε is a Gaussian random vector with a zero mean computed from the approximation errors in error equation. Since X and Y are Gaussian random vectors, a new random vector Z can be defined as $Z_{m \times 1} = [X^T Y^T]^T$. Then, the pdf of Z is equivalent to the joint pdf of X and Y , which can be computed as shown in (24) [8]:

$$f_Z(Z) = f_{X,Y}(X,Y) = \frac{\text{Exp}\{-1/2([Z] - E[Z])^T [\text{Cov}(Z)]^{-1} ([Z] - E[Z])\}}{(2\pi)^2 |\text{Cov}(Z)|^{1/2}} \quad (24)$$

where $E[Z] = [\mu_X^T \mu_Y^T]^T$, and $\text{Cov}(Z)_{n \times n}$ is a matrix composed of covariance matrices as shown in [8]. Note that for independent design parameters, $\text{Cov}(X, X)$ is the diagonal matrix of parameter variances. The expected value of the conditional pdf in (22) can be computed as [8]:

$$E[X|Y=y] = \mu_X + \text{Cov}(X,Y)[\text{Cov}(Y,Y)]^{-1}(Y - \mu_Y) \quad (25)$$

8.1 Diagnosis of Dualband Filter

The dualband filter design shown in Fig.4 has been used for multi-domain statistical analysis and diagnosis. A vector of layout parameters with random values was chosen according to their statistical distribution and was modeled and simulated. The resulting performance measures were $\min_attn=1.9933$ dB, $\text{ripple}=0.6513$ dB and f_2 (higher side of 1 dB frequency) = 2.5342 GHz. For this filter, the center frequency was shifted. Table I shows the simulated and estimated manufacturing variations. It is clear that the diagnosis technique do not give the *exact* statistical variation of layout parameters in batch fabrication, but it captures the dominant variations. The results of statistical distributions show good correlation with results using Monte Carlo methods. However, with the extensive EM simulations on layouts and having statistical distributions on all the layout parameters, Monte Carlo simulations took 36 hours on a DELL PC with 2.6 GHz processor and 1 GB RAM.

TABLE I

Layout parameter	Random Input parameters	Estimated parameters	Least squares
Resn_L	$\mu+2.29\sigma$	$\mu+2.26\sigma$	$\mu+1.52\sigma$
C_resn	$\mu-1.34\sigma$	$\mu-1.66\sigma$	$\mu-3.95\sigma$
C_mid	$\mu-0.71\sigma$	$\mu-0.35\sigma$	$\mu-6.64\sigma$
C_match	$\mu+1.92\sigma$	$\mu+2.27\sigma$	$\mu+2.76\sigma$

9. YIELD OPTIMIZATION

The probability density functions that represent the variations in design parameters are Gaussian in nature. The design yield, which is computed as an integral of the joint probability density, can therefore be posed as a convex programming problem. The joint Gaussian pdf of n random independent variables $y=(y_1, \dots, y_n)$ where y_i has mean x_i and variance σ_i , is given by

$$\Phi_x(y) = \frac{1}{(2\pi)^{n/2} \sigma_1 \sigma_2 \dots \sigma_n} \exp \left[-\sum_{i=1}^n \frac{(y_i - x_i)^2}{2\sigma_i^2} \right] \quad (26)$$

where $x=(x_1, \dots, x_n)$. The above joint distribution is known to be a log-concave function of x and y . Further, arbitrary covariance matrices can be handled, since a symmetric matrix can be converted to the diagonal form by use of orthogonal transformation. The optimization problem is formulated as

$$\text{maximize } Y(x) = \int_P \Phi_x(y) dy \quad \text{such that } x \in P$$

where P is the approximation to the feasible region. Since the integral of a log-concave function is also a log-concave function, the problem reduces to maximization of a log-concave function over a convex set. In this problem, the local minimum is the global minimum. The algorithm proposed in [13] provides an efficient technique for solving a convex programming problem. The algorithm consists of iteratively finding centers of approximated "polytopes" which constitute the feasible region. Since the yield function is not available in an explicit form, the gradient is estimated using yield gradient approximation methods. This is computationally much cheaper than repeated circuit/EM simulations with new sets of parameter values. An approximate estimate (based on a sample of N points) for yield, based on the gradient function as [13]:

$$\frac{\partial \hat{Y}}{\partial x_i} = \frac{1}{N} \sum_{k=0}^N \frac{g(z_k)}{\Phi_x(z_k)} \frac{\partial \Phi_x(z_k)}{\partial x_i} \quad (27)$$

where $g(z)=0$ where $z \notin P$ and $g(z)=1$ when $z \in P$. The results of optimization have been shown in Table II. The table shows the change in the mean of the performance measures as a result of the optimization of the design parameters. A yield improvement of ~14% has been observed based on the aforementioned analysis.

TABLE II

Perf. Metric Mean	Initial estimate	Optimized Estimate
μ IL (dB)	2.03	2.18
μ BW (GHz)	0.225	0.242
μ attn(dB) @3.5 GHz	35	30
μ fc2 (GHz)	0.252	0.267

10. CONCLUSION

The recent trend for high-performance multilayer RF circuits demands for improved design/diagnosis methods to reduce design-cycle time. A multi-domain statistical analysis and diagnosis methodology for LCP based RF circuits has been presented. The methods have been confirmed by limited measurement and extensive EM data. Multiple runs of fabrications are being carried out for extensive validation. Further, the effect of the properties of copper with thermal cycling and humidity will also be investigated. The lumped-element modeling approach shows limitations beyond 4-5 layers. Further, the time for generation and accuracy of sensitivity analysis data becomes the bottleneck to fast design cycle of compact layouts with large number of passives (>20). Misalignment between layers is critical to performance of stacked inductors which is being currently investigated. Development of physics-based reliability models to relate component variation/failure mechanisms to system-level performance require tremendous resources and time. Simplified, multi-domain, semi-analytical models are shown to be necessary to ease the computational complexity and achieve acceptable results, thereby leading to reduced design effort.

11. REFERENCES

- [1] M.A.Styblinski, "Statistical design centering approach to minimax circuit design", in *Proc. IEEE Int. Symp Circuits and Syst.*, Portland, OR, May 1989, pp-697-700.
- [2] S.Sapatnekar, P.M.Vaidya and S.M.Kang "Convexity-based algorithms for design centering", *IEEE Trans. on Computer-Aided Design*, vol.13, pp.1536-1549, Dec. 1994.
- [3] K.S.Tahim and R.Spence, "A radial exploration approach to manufacturing yield estimation and design centering", *IEEE Trans. Circuits Syst.*, vol. CAS-26, pp.768-774, Sept. 1979.
- [4] K.Choi et.al., "Post-optimization design centering for RF Integrated Circuits", in *Proc. IEEE Int. Symp. Circuits and Syst.*, Vancouver, Canada, May 2004, pp.956-959.
- [5] H.L.Malek and A.Hassan, "The ellipsoidal technique for design centering and region approximation", *IEEE Trans. on Computer-Aided Design*, vol.10, pp.1006-1014, Aug. 1991.
- [6] V.Govind, S.Dalmia and M.Swaminathan, "Design of LNA using embedded passives in organic substrates," *Trans. Adv. Packag.*, vol. 27, pp. 79-89, Feb. 2004.
- [7] A. Bavisi, S. Dalmia, M. Swaminathan, G. White, and V. Sundaram, "Chip-package co-design of integrated voltage controlled oscillator in LCP substrate," accepted for publication at *IEEE Trans. Adv. Packag.*, 2005.
- [8] S.Mukherjee, M.Swaminathan and E.Matoglu, "Statistical analysis and diagnosis methodology for RF circuits in LCP substrates," *IEEE Trans, Microwave Theory Tech.*, vol.53, no.11, pp.3621-3630.
- [9] S.Suresh, *Fatigue of Materials*, Cambr. Univ. Press, 2nd ed.
- [10] M.Damani et. al, "Physics-based reliability assessment of embedded passives," *2004 Electronic Components and Technology Conf.*, pp. 2027-2031.
- [11] A.I.Khuri, *Response Surfaces*, New York: Marcel Decker '87.
- [12] G.R.Cooper and C.D.McGillem, *Probabilistic methods of signal and system analysis*, New York; Holt, 1971.
- [13] P.M.Vaidya, "A new algorithm for minimizing convex functions over convex sets," *Proc. IEEE. Fundamentals of Computer Science*, pp. 332-337, Oct. 1989.